Hindawi
Advances in Civil Engineering
Volume 2022, Article ID 5908317, 11 pages
https://doi.org/10.1155/2022/5908317

Research Article

Optimization Analysis of Mechanical Properties of Fly Ash-Based Multicontent Gasification Slag Paste Filling Material

Denghong Chen,[1,2] **Tianwei Cao**,[1,2] **Ran Chen**,[1,2] **and Chao Li**[1,2]

[1]*School of Mining Engineering, Anhui University of Science and Technology, Huainan 232001, China*
[2]*Institute of Energy, Hefei Comprehensive National Science Center, Anhui, Hefei 230031, China*

Correspondence should be addressed to Denghong Chen; dhchen@aust.edu.cn

Received 9 January 2022; Accepted 20 January 2022; Published 30 March 2022

Academic Editor: Bing Bai

Copyright © 2022 Denghong Chen et al. This is an open access article distributed under the Creative Commons Attribution License, which permits unrestricted use, distribution, and reproduction in any medium, provided the original work is properly cited.

In view of the difficult utilization of a large amount of coal-based solid waste produced by coal electrification in the Ningdong mining area, especially the large storage and low utilization rate of gasified slag, combined with the advantages of high paste filling concentration, fast efficiency, and low construction cost, it is of great significance to study the appropriate proportion of fly ash-based multicontent gasified slag paste filling material for green mining and large-amount utilization of gasified slag. Based on the microstructure, composition, and particle size distribution of gasification slag, fly ash, broken coal gangue, furnace bottom slag, and desulfurization gypsum tested by XRD, SEM, and particle size sorting screen, the mass fraction (X_1), gasification slag content (X_2), *m* (c): *m* (FA) (X_3). 29 groups of schemes are designed by four factors : mass fraction X_1 refers to the proportion of solid in the filling paste, the amount of gasification slag in the solid X_2 refers to the proportion of gasification slag in the solid, and m (c): m (FA) X_3 refers to the proportion of fly ash and cement in the solid excluding gasification slag, coal gangue, desulfurization gypsum, and furnace bottom slag. The amount of desulfurization gypsum in the solid X_4 refers to the proportion of desulfurization gypsum in the solid. The flow and strength characteristics of each group are analyzed. It is found that before proportioning, coal gangue of 2.5~5 mm accounts for 80.8%, furnace bottom slag of less than 2.5 mm accounts for 56.5%, fly ash of 20~80% μm accounts for 80%, and fly ash of 10~20% μm accounts for 90%. XRD patterns reveal that the main components of four solid wastes and cement are SiO_2 and Ca_3SiO_5, and the chemical composition of desulfurization gypsum is $Ca(SO_4)(H_2O)_2$. The regularity of size change tends to be consistent, and the uniaxial compressive strength of 3 days later in group thirteenth exceeds 0.991 MPa. Combined with the flow characteristics, it is determined that there are 6 optimization groups in the inclined ladder area with the expansion of 200~250 mm and the uniaxial compressive strength of 0.6~1.4 MPa. The compressive strength increases with the increase of the mass fraction of single-factor analysis. The response surface method of C shows that the significance of X_1, X_2, X_3, and X_4 decreases in turn. The central combination design is used to predict that the mix proportion of X_1 is 84%, X_2 is 15%, X_3 is 1 : 5, and X_4 is 7%, the content of coal gangue is 10%, and the content of furnace bottom slag is 5% which is the best. The supplementary experimental results show that σ_{3d} is 1.35 MPa and the expansion is 200 mm. Combined with SEM, it is found that the microstructure before and after optimization is rich in hydration products and the internal structure is well cemented, which further explains σ_C. The above research provides important basic parameters for large-scale disposal and green filling mining which is difficult to deal with a large amount of stockpiled gasification slag.

1. Introduction

At present, the main body of energy utilization in China is coal. Coal gangue, fly ash, desulfurization gypsum, and coal gasification slag produced in the process of coal mining and utilization are common coal-based solid wastes. According to incomplete statistics, the annual output of coal-based solid waste is about 1.5 billion tons, accounting for more than half of the output of industrial solid waste. At present, the comprehensive utilization of coal-based solid waste is still limited. In this way, the utilization status in the form of temporary storage will not only cause serious environmental pollution problems, such as the occupation and waste of land resources caused by open-air storage and the impact of floating dust on the quality of

the atmospheric environment, but also cause the harmful substances in coal-based solid waste enter the surface water body and penetrate into the ground with rainwater, polluting the water environment. It causes certain potential safety hazards to a human living environment. [1] Taking Ningdong mining area as an example, the output of solid waste increased from 4.4 million T to 24 million T from 2010 to 2020, of which the output of coal gasification slag has exceeded 7 million T, mostly buried and stacked in the open air (Figure 1, coal electrification base). Due to the high cost of treatment and utilization of solid wastes such as gasification slag and great technical difficulty, the comprehensive utilization rate of solid wastes in Ningdong base was only 28.9% in 2018 and the utilization rate of gasification slag was low [2]. The total amount of ash and slag in the Ningdong area is very large, with an annual emission of nearly 20 million tons, mainly including fly ash, coal chemical gasification ash, desulfurization gypsum, coal gangue, of which coal chemical gasification ash and fly ash account for the largest proportion [3]. The research on the utilization of gasification slag mainly focuses on the preparation of building materials, soil improvement, and water restoration, separation and utilization of residual carbon, preparation of catalyst carriers and ceramic materials, preparation of silicon-based materials, etc. [4]. At present, the application is relatively single and the degree of effective treatment is not high. Its treatment will not only increase the transportation cost but also cause environmental problems such as land occupation and dust pollution [5]. Many scholars have made many research achievements on the utilization of gasified slag. Shen Wang, Cheng Zhenyun, and Chen Haixia tested the fresh mixing performance of alkali-activated gasified slag fly ash cement mortar with the substitution rate of gasified slag of 0%, 10%, 20%, and 30%, respectively, and the physical and mechanical properties of alkali-activated gasified slag fly ash mortar under two different curing conditions of 20°C and 60°C, respectively. However, the improvement of mechanical properties is strongly dependent on conditions, which has an impact on the disposal of a large amount of gasification slag; Ma Chao et al. studied the ammonia nitrogen adsorption performance of the bulk coal gasification slag produced in the coal gasification process after separation by a water-based cyclone, but the process is complex and the utilization rate is limited. Zhao Aijing et al. use coal-based solid wastes such as gasification slag as a silicon source and aluminum source to prepare nanoporous materials with high added value. There are few studies on the influence of many factors such as high cost and performance stability. In order to prepare nanoporous materials with high added value, there are few studies on the influence of many factors such as high cost and performance stability. At the same time, the mining of coal resources by the full caving method also has a serious impact on surface subsidence and water and soil loss. In conclusion, it is urgent to study the green filling materials with high content of gasified slag, high strength, and good fluidity, so as to meet the low construction cost and large-scale disposal of a large amount of gasified slag stored in the Ningdong mining area. This paper intends to use a variety of research methods to analyze the microstructure and physicochemical properties of filling raw materials, obtain the particle size of fly ash and cement with a laser particle size analyzer, analyze the composition of multisource coal-based solid waste by X-ray diffraction technology, and design by the response surface method. The filling matching scheme is designed by response surface method, which is mainly composed of multi-content gasified slag and supplemented by fly ash content, m (c): m (FA) and desulfurization gypsum content. The regularity of single factor on the early strength of filling materials is analyzed by considering the influence of four factors: solid mass fraction, multi content gasified slag, m (c): m (FA), and desulfurization gypsum content on the early strength of filling materials; the regularity of single factor on the early strength of the filling material is analyzed and the suitable filling mix proportion scheme is limited in combination with the flow characteristics. The influence ranking of X_1, X_2, X_3, and X_4 is obtained by the response surface method of σ_C, and the optimal ratio is predicted by using the central combination design, which provides a new path for the multicontent gasification slag solid waste filling material with low utilization rate and difficult disposal.

2. Main Components and Particle Size Distribution of Coal-Based Solid Waste in the Ningdong Area

In this paper, fly ash-based gasification slag with high content is taken as the main research object, supplemented by coal gangue, desulfurization gypsum, and furnace bottom slag, and then mixed with ordinary 42.5 Portland cement to prepare green filling material [6]. The microcomponents of the five solid wastes were analyzed using a SmartLab X-ray diffractometer (XRD) to analyze the mineral phase of the raw materials (equipment parameters: angle of 5°~65°, scanning speed of 10°/min). Under these conditions, the XRD main components of the five coal-based solid wastes shown in Figure 2 were obtained. The micromorphology of coal-based solid waste was observed by daily FLEXSEM 1000 SEM. Under the condition of accelerating voltage of 10.0 kV, the microstructure of coal-based solid waste raw material and filling material cement was obtained. The experimental instruments used are shown in Figure 3.

The main mineral phase of gasification slag is quartz SiO_2, which contains trace heavy metal element arsenic. The main mineral phase of fly ash is SiO_2. The main mineral phase of desulfurized gypsum is $Ca(SO_4)(H_2O)_2$. The main mineral phase of furnace bottom slag is SiO_2 [7]. The main mineral phases of cement are calcium silicate and tricalcium silicate Ca_3SiO_5, which determine its early strength [8].

2.1. Gasification Slag. The gasification slag is taken from the coal to oil branch of Ningxia coal industry group, Ningdong coal power base. The gasification slag is the waste slag generated in the production process of the gasifier.

2.2. Fly Ash. The fly ash used in this experiment comes from the coal to oil branch affiliated to the Ningxia coal industry group. The fly ash used belongs to fine external ash with a small particle size. The particle size measured with the laser particle size analyzer is mainly less than 200 μm (Figure 4(c)), of which 20~80 μm particles of M account for

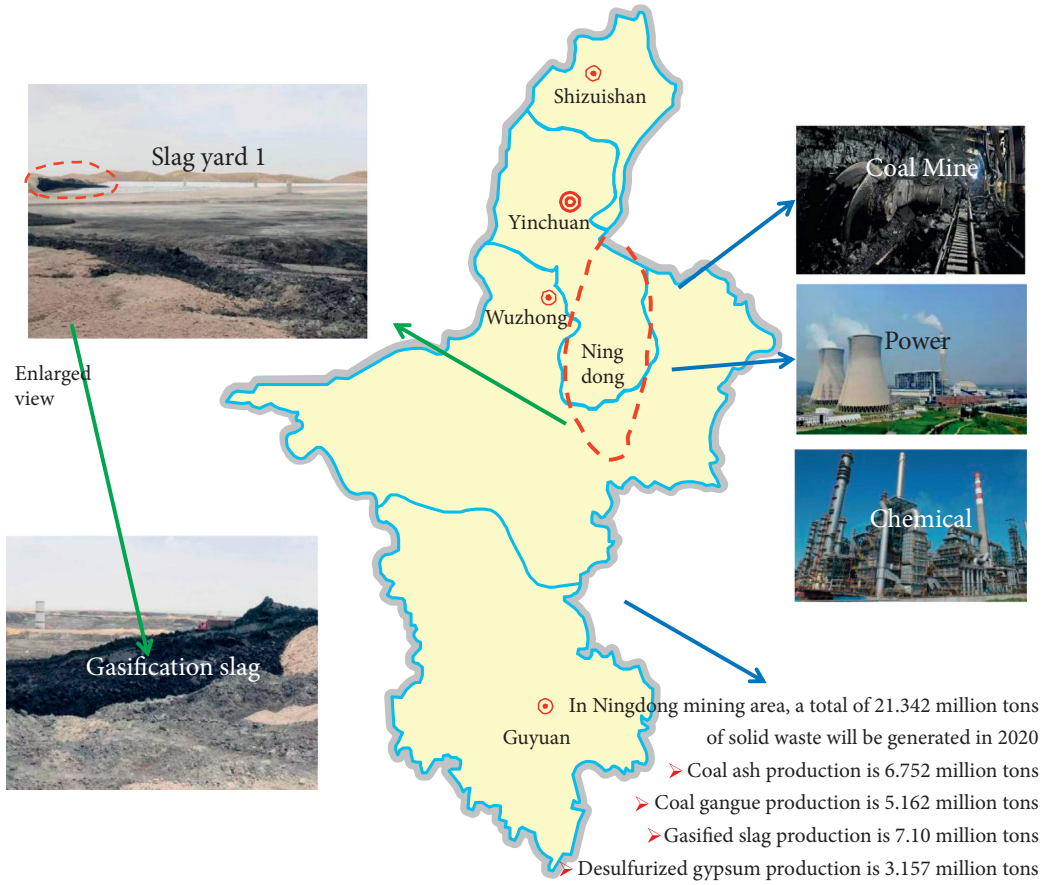

Figure 1: Analysis of coal-based solid waste output in the Ningdong mining area.

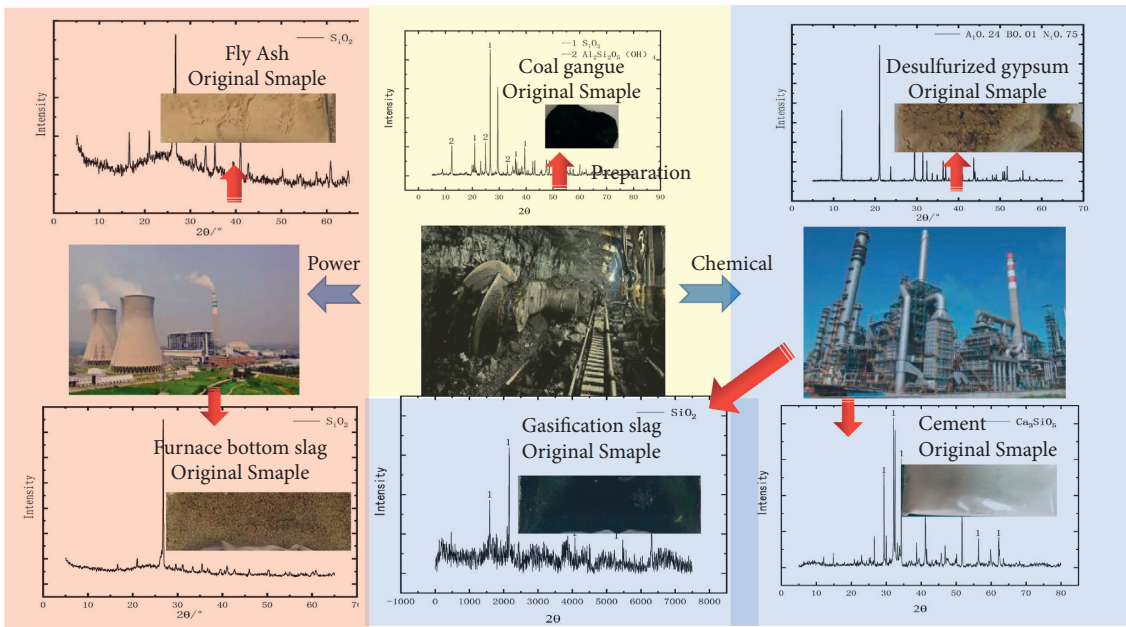

Figure 2: XRD spectra of five solid wastes in the Ningdong mining area.

(a) (b) (c)

Figure 3: Microstructure and composition analysis instrument. (a) X-ray diffractometer. (b) SEM. (c) Laser particle size analyzer.

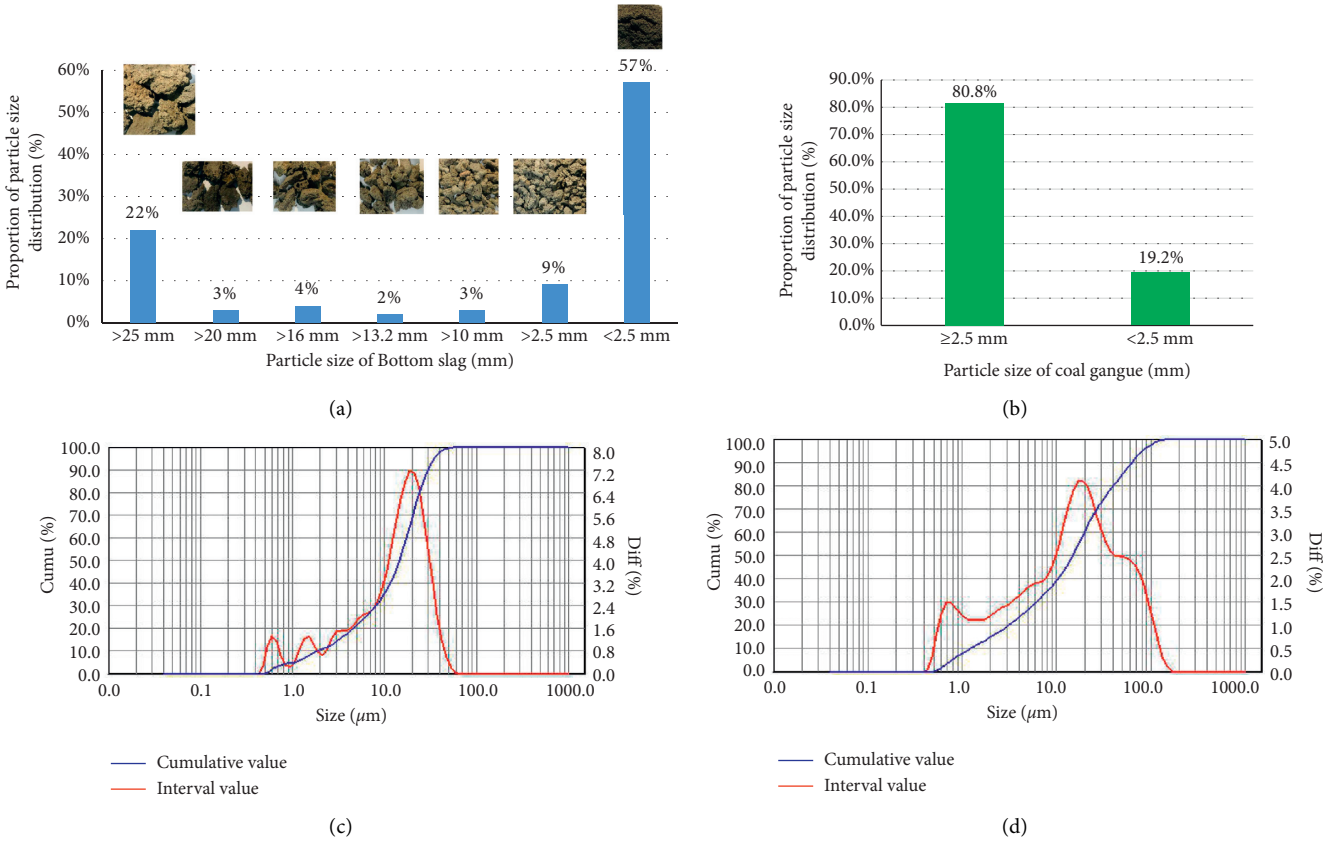

Figure 4: Statistical analysis of particle size distribution of furnace bottom slag, broken coal gangue, and fine particle raw materials before proportioning experiment. (a) Furnace bottom slag. (b) Coal gangue. (c) Fly ash. (d) Cement.

the majority and they are fine particles. When combined with the aggregate, it is conducive to improving the early strength of the consolidated body.

2.3. Desulfurized Gypsum. The desulfurized gypsum is taken from the coal to oil branch of Ningxia coal industry group, Ningdong coal power base, and is an earthy yellow viscous block.

2.4. Coal Gangue. The coal gangue is taken from Renjiazhuang coal mine affiliated to Ningxia coal industry group, Ningdong coal power base, and is a gray-black block. At the same time, according to the method [9] specified in the standard for geotechnical test methods 1, the two-stage jaw crusher is used to crush the coal gangue to about 2.5 mm. After grading and screening 6 kg of crushed coal gangue by the sieve analysis method, its particle size distribution is as shown in Figure 4(b).

2.5. Furnace Bottom Slag. The furnace bottom slag is taken from the coal to oil branch affiliated to Ningxia coal industry group in the Ningdong coal power base. The furnace bottom slag is the waste slag generated in the production process of

2 kg of gasifier. Original furnace bottom slag is graded and screened by the screening method. The particle size distribution is shown in Figure 4(a). It is used randomly in the experiment.

3. Analysis of Proportioning Results of Coal-Based Solid Waste Filling Materials

3.1. Experimental Scheme. Based on the understanding of the main components and particle size distribution of five kinds of solid wastes, the research on the mix proportion optimization of fly ash-based filling materials with multicontent gasification slag is carried out. We prepare multisource solid waste paste filling materials with a large amount of gasified slag, with good fluidity and high strength, so as to realize the combination of a large amount of coal-based solid waste [10], especially the solid waste consumption of a large amount of stacked gasified slag (7.1 million tons of gasified slag in the Ningdong area in 2020) [11] and green filling mining [12]. The experiment used $70.7 \times 70.7 \times 70.7$ mm triple standard mold. Due to the low utilization value and difficult treatment of gasification slag in the Ningdong base mining area, it is mainly mixed with more gasification slag. In addition, considering the compressive strength of the filling body, different levels of cement and a small amount of desulfurization gypsum are used to study their influence on the compressive strength. In this experiment, coal gangue with a particle size of 2.5–5 mm after secondary jaw crushing is used. Considering that the crushing cost of bulk coal gangue is too high, there is no too much research on coal gangue, furnace bottom slag, and other relatively easy-to-dispose solid wastes, supplemented by desulfurization gypsum, coal gangue, furnace bottom slag, and fly ash. The experimental factors and levels are shown in Table 1 [13]. The content of fixed bottom slag is 5%, and the content of coal gangue is 10%. Here, C : FA = cement : fly ash.

According to the requirements of strength test standards, the gasification slag is used as a multicontent raw material through the flow chart (Figure 5), mixed with fly ash, desulfurization gypsum, furnace bottom slag, and coal gangue and evenly stirred for 180 s to make a $70.7 \times 70.7 \times 70.7$ mm specimen which shall be taken out after reaching the testing age of 3 d, 7 d, and 14 d, and the uniaxial compressive strength test of the specimen shall be completed on the RMT testing machine [14].

3.2. Experimental Results and Single-Factor and Two-Factor Analysis. The response surface experimental design scheme and results are shown in Table 2. Using Box–Behnken design expert software, 29 groups of filling material proportioning experimental schemes with four factors and three levels are designed, and the response surface function relationship of early compressive strength of paste at 3 d age is established.

$$R_{3\,d} = 0.99 - 0.089X_1 + 0.24X_2 - 0.076X_3 + 0.057X_4. \quad (1)$$

Through the compressive strength test of multiple groups of proportioned test blocks at different ages on the RMT testing machine, the change trend of compressive strength of the same group of proportioned test blocks at different ages can be obtained. At the age of 3 d, 7 d, and 14 d, the change law of uniaxial compressive strength of the same proportion number tends to be consistent, and the compressive strength of filling materials increases with the increase in age, as shown in Figure 6(a). The mean value of uniaxial compressive strength of 29 groups of proportioned test blocks at the age of 3 d, 7 d, and 14 d is calculated, and the calculation result is $\overline{R}_{3\,d} = 0.991$ MPa, $\overline{R}_{7\,d} = 1.411$ MPa, and $\overline{R}_{14\,d} = 2.107$ MPa.The stress-strain curves of high- and low-strength test blocks are obtained, as shown in Figure 6(b). It can be concluded that there are 13 groups of high-strength proportion at 3d age, and the specific proportion number is as follows: 3, 4, 5, 7, 9, 11, 14, 16, 17, 18, 22, 23, and 24. The results show that the mass fraction has the highest influence on the early compressive strength of paste filling materials, and it has a positive correlation with the early compressive strength. The higher the mass fraction concentration, the higher the 3 d uniaxial compressive strength and the higher the influence on the later compressive strength. When the mass fraction is 80%, the strength is distributed as follows: X_4 has the least effect on compressive strength. X_1 has a negative correlation with the compressive strength, X_2 and X_3 have a positive correlation with the compressive strength, and X_4 has the characteristic of slow increase in the early compressive strength of the filling material. The increase in the gasification slag contentcan inhibit the increase in compressive strength. With the increase in mass concentration and cement content, the compressive strength increases gradually.

Table 1: Factors and levels in the design scheme of the central composite experiment.

Factor	Level		
	−1	0	1
$X1$ (mass fraction/%)	75	80	85
$X2$ (content of gasification slag in solid/%)	15	20	25
$X3$ (m(c):m(FA))	1 : 5	1 : 6	1 : 7
$X4$ (content of desulfurized gypsum in solid/%)	6	9	12

Combined with the high concentration paste filling technology [15], in order to better adapt to the current situation of bulk coal-based solid waste disposal in the Ningdong mining area, considering that the filling material has relatively good fluidity and provides large flow transportation for underground filling, in this paper, the suitable expansion of paste filling material is 200–250 mm [16] and the compressive strength of filling material is 0.6–1.4 MPa. The inclined step area obtained is circled according to the relevant parameters of uniaxial compressive strength and fluidity, so as to obtain the best ratio in this range, as shown in Figure 7. It can be seen from the figure that the six groups of filling materials with ratios 4, 11, 16, 18, 20, and 22 are the best under the interaction of uniaxial compressive strength and fluidity, as shown in Table 3.

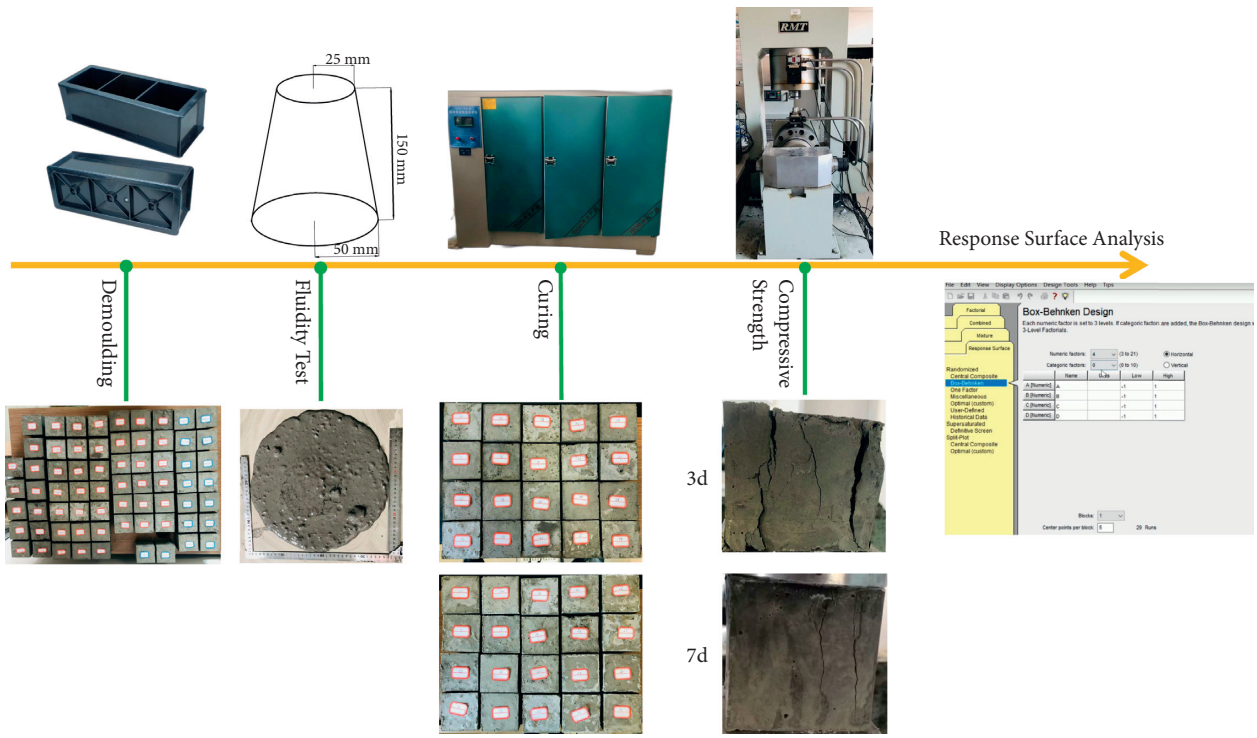

Figure 5: Test flow chart of coal-based solid waste filling material.

Table 2: Response surface design and results.

No.	Level				Early compressive strength (MPa)			No.	Level				Early compressive strength (MPa)		
	X_1	X_2	X_3	X_4	3 d	7 d	14 d		X_1	X_2	X_3	X_4	3 d	7 d	14 d
1	−1	−1	0	0	0.544	0.868	2.4	16	0	1	1	0	1.404	2.173	3.3
2	1	−1	0	0	0.588	0.704	1.2	17	−1	0	−1	0	1.380	1.673	2.6
3	−1	1	0	0	1.252	1.877	2.3	18	1	0	−1	0	1.016	1.200	1.8
4	1	1	0	0	1.468	2.153	3.5	19	−1	0	1	0	0.936	1.032	1.2
5	0	0	−1	−1	1.080	2.141	3.1	20	1	0	1	0	0.740	0.844	0.9
6	0	0	1	−1	0.908	1.548	3.5	21	0	−1	0	−1	0.736	0.848	0.9
7	0	0	−1	1	1.032	1.929	3.1	22	0	1	0	−1	0.992	1.092	2.1
8	0	0	1	1	0.748	1.232	2.6	23	0	−1	0	1	1.588	2.561	2.6
9	−1	0	0	−1	1.256	2.197	4.1	24	0	1	0	1	1.460	2.157	2.2
10	1	0	0	−1	0.920	1.204	1.8	25	0	0	0	0	0.876	1.236	1.9
11	−1	0	0	1	1.088	1.348	1.5	26	0	0	0	0	0.932	1.312	1.5
12	1	0	0	1	0.656	0.812	1.1	27	0	0	0	0	0.764	1.180	1.7
13	0	−1	−1	0	0.712	0.760	1.2	28	0	0	0	0	0.984	1.164	1.6
14	0	1	−1	0	1.072	1.753	3.0	29	0	0	0	0	0.976	1.304	1.6
15	0	−1	1	0	0.640	0.608	0.8	Response surface design method-central combination design method							

4. Analysis and Discussion of the Response Surface Method Model

4.1. Model Analysis and Significance Evaluation under Response Surface Methodology. Based on the significance of the influence between the factors of the response surface regression model and the response value, the error source of the model equation is analyzed [17]. The importance of the model is determined by F and P values. The larger the F value is, the smaller the P value is and the more significant the influence is [18]. The F value of the established regression model is 3.86, which shows that the regression effect of the model is remarkable, and the model fits the experimental values well. The significance of single factor is $X_1 > X_2 > X_3 > X_4$. The model is used to determine the correlation coefficient to evaluate the accuracy and reliability of the regression model. The larger the F value of each factor, the more significant it is, as shown in Table 4. The model judgment correlation coefficient interprets the difference between the response surface and the real value [19] and analyzes the fitting degree of each model of the response surface method. The

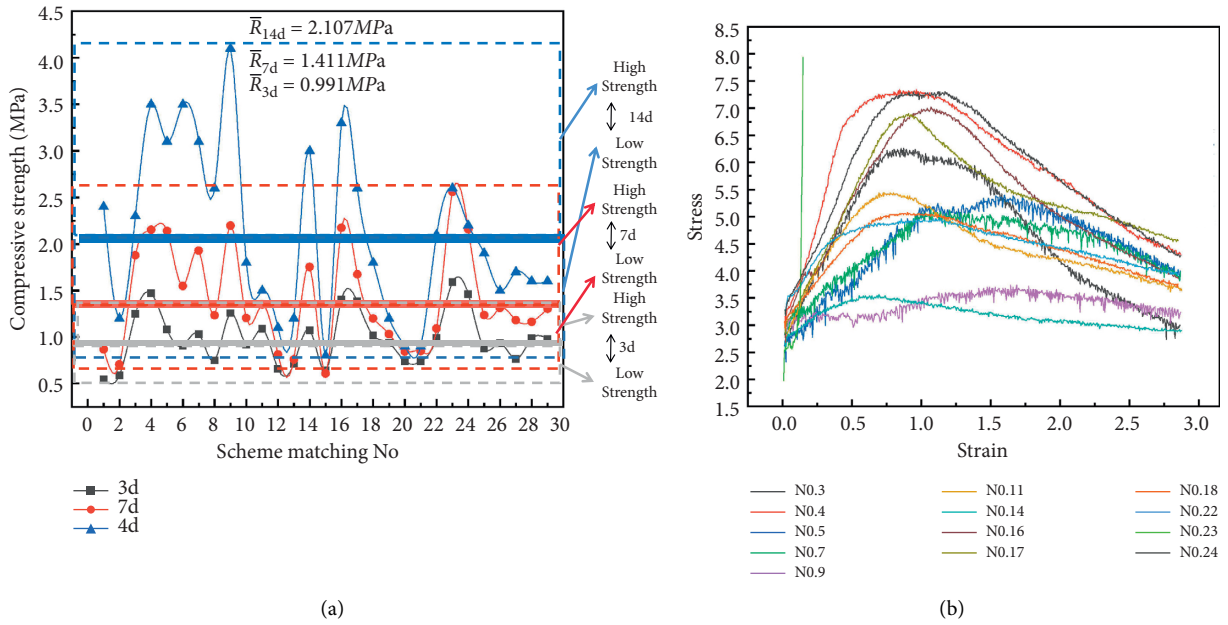

(a) (b)

Figure 6: Change in compressive strength at different ages. (a) Compressive strength at different ages. (b) Stress-strain curve of the high-strength test block.

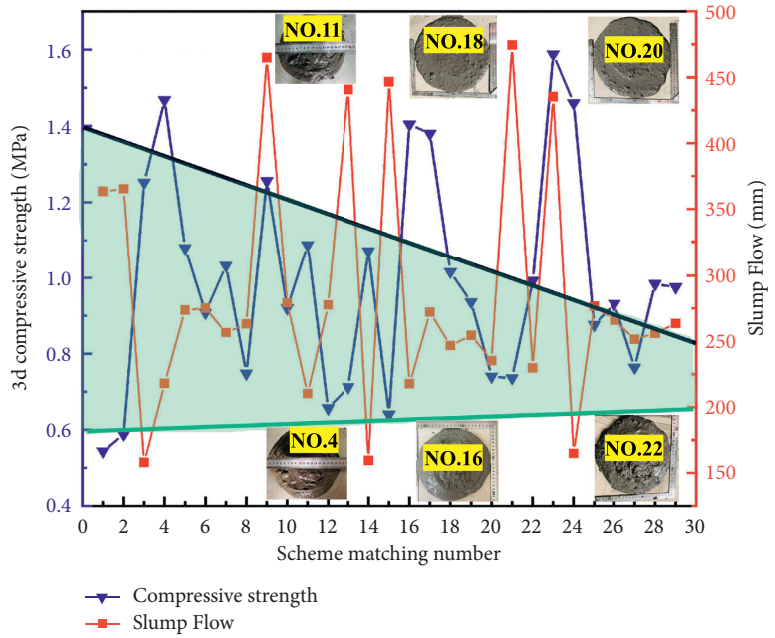

Figure 7: Interaction diagram of compressive strength and expansion at different ages under different proportion numbers.

Table 3: Optimization of and expansion under different compressive strengths.

Matching number	Ratio number factor parameter	3 d uniaxial compressive strength (MPa)	Degree of expansion (mm)
4	$X1 = 25\%$; $X2 = 85\%$; $X3 = 1:6$; $X4 = 9\%$	1.468	218
11	$X1 = 15\%$; $X2 = 80\%$; $X3 = 1:6$; $X4 = 12\%$	1.088	210
16	$X1 = 20\%$; $X2 = 85\%$; $X3 = 1:7$; $X4 = 9\%$	1.404	217.5
18	$X1 = 25\%$; $X2 = 80\%$; $X3 = 1:5$; $X4 = 9\%$	1.016	246.5
20	$X1 = 25\%$; $X2 = 80\%$; $X3 = 1:7$; $X4 = 9\%$	0.740	235
22	$X1 = 20\%$; $X2 = 85\%$; $X3 = 1:6$; $X4 = 6\%$	0.992	229.5

Table 4: Analysis of variance of experimental results of the linear model.

Source	Sum of squares	Mean square	F value	P value
Model	0.88	0.22	3.86	0.0147
X_1	0.095	0.095	1.68	0.2077
X_2	0.67	0.67	11.85	0.0021
X_3	0.07	0.07	1.23	0.2778
X_4	0.039	0.039	0.68	0.4178
Residual	1.36	0.057		
Lack of fit	1.33	0.066		
Pure error	0.033			

Table 5: Analysis of the fitting degree of each model by the response surface method.

Model source	R^2 correction value	R^2 estimate	Remarks
Linear model	0.3915	0.0618	Recommended
2FI model	0.4352	Negative	
Cubic model	0.9344	Negative	

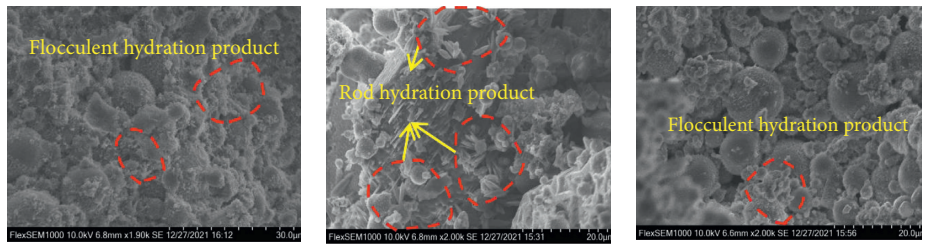

(a) (b) (c)

Figure 8: SEM of the typical filling material test block. (a) SEM hydration products of No. 18 filling material. (b) SEM hydration products of No. 4 filling material. (c) SEM hydration products of No. 20 filling material.

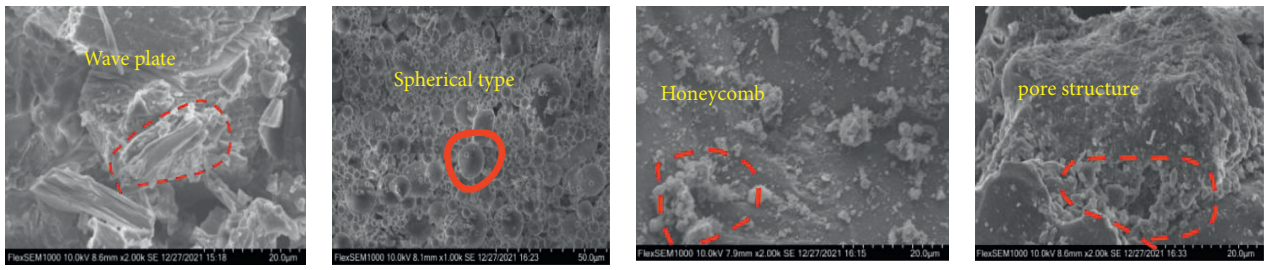

(a) (b) (c) (d)

Figure 9: SEM structure before multisource coal-based solid waste proportioning experiment. (a) Desulfurized gypsum. (b) Fly ash. (c) Gasification slag. (d) Furnace bottom slag.

evaluation results are shown in Table 5. The closer the correlation coefficient is to 1, the higher the reliability of the model is. The complex correlation coefficient is 0.3915, and the prediction correlation coefficient is 0.0618, which proves that the model has high accuracy. The contour line and 3 d response surface of the multiple regression equation of the linear model represent the interaction results of each factor. It can not only predict and optimize the response value but also analyze any single factor to obtain the significance law [20].

4.2. Discussion. From the uniaxial compressive strength and fluidity-related parameters, three typical representative test blocks with ratios 4, 18, and 20 are circled in the inclined ladder area. After cementation, the hydration reaction is severe. The SEM microstructure shows the abundance of rod and flocculent hydration products, which have different promoting effects on the compressive strength of filling materials (Figures 8(a)–8(c)). The microstructure of raw materials used for filling is shown in Figures 9(a)–9(d). Through the comparison of

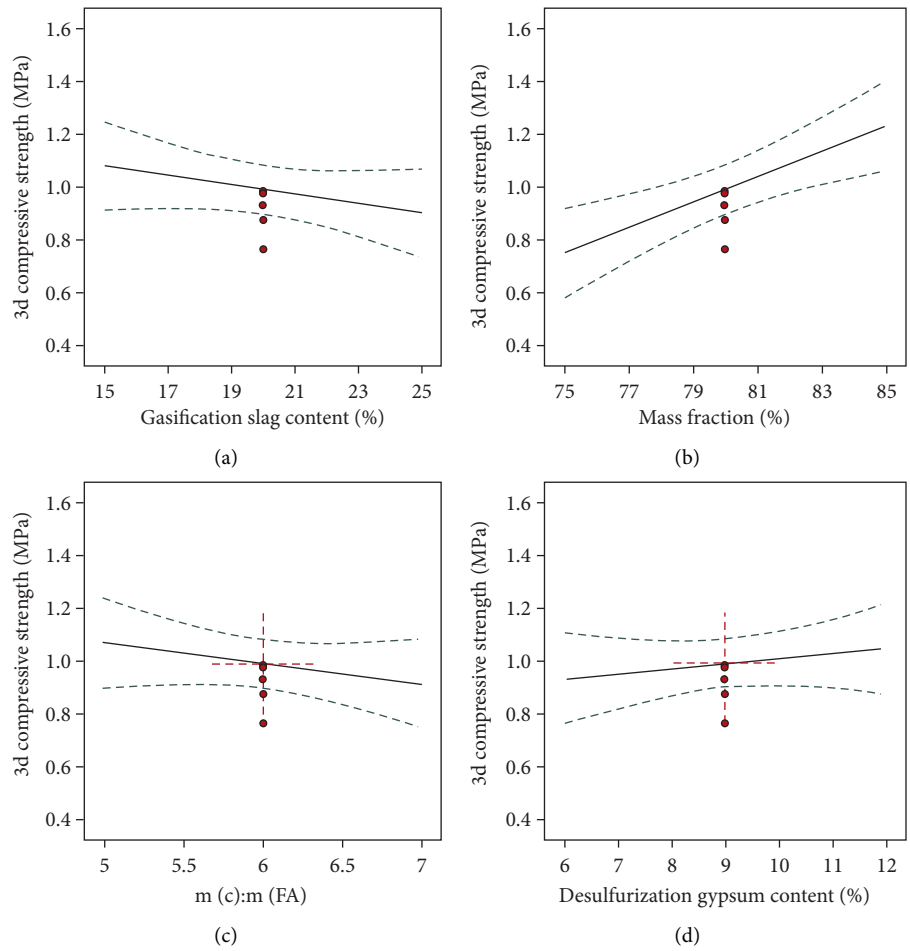

Figure 10: Prediction of single-factor effect on 3 d uniaxial compressive strength response surface. (a) X_1 single-factor influence prediction. (b) X_2 single-factor impact prediction. (c) X_3 single-factor impact prediction. (d) X_4 single-factor impact prediction.

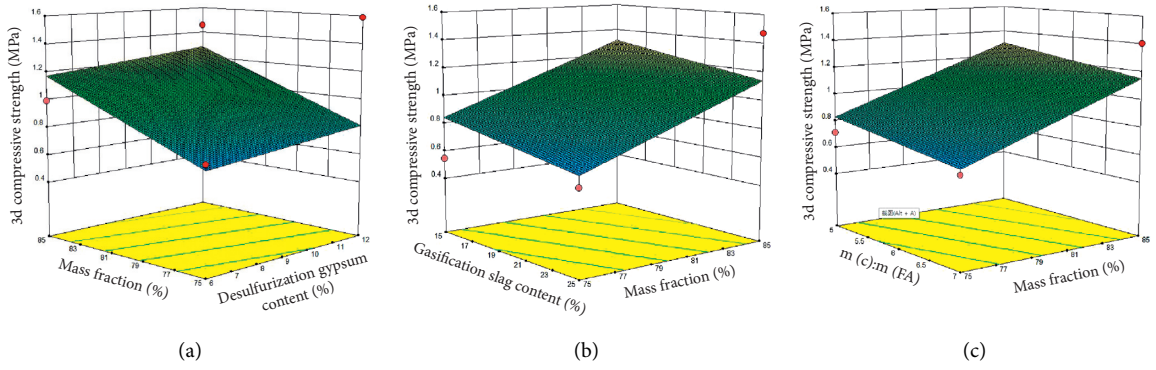

Figure 11: Analysis of interaction factors of 3 d uniaxial compressive strength response surface. (a) X_2X_4 interaction cloud. (b) X_1X_2 interaction cloud. (c) X_2X_3 interaction cloud.

the structure between the filling body and the filling body raw materials, we can clearly see that there are different quantities of hydration products in the filling body, which bond the interior of different raw materials together and have a certain compressive strength.

A variety of coal-based solid wastes are mixed and cemented. Compared with the original microstructure of various solid wastes, the hydration products produced by hydration reaction under the action of cement are different. The early strength of the filling body is mainly due to the hydrolysis reaction and hydration reaction of cement, and the free water becomes bound water. Cement forms cementitious material through a series of chemical reactions to increase its strength. The chemical reaction of the active

components of gasification slag is slow, the hydration products formed in the early stage are less, and the strength is low. Abundant multiform hydration products can promote the compressive strength of filling materials, and the law of compressive strength is demonstrated.

In addition, in order to intuitively study the correlation law of fly ash, coal gasification slag, coal gangue, and cement content on the early compressive strength of the filled consolidated body, the contour map and response surface cloud map of compressive strength varying with factor levels are drawn according to the regression model, as shown in Figures 10 and 11, respectively. According to the results of variance analysis of single-factor and multifactor interaction in Table 5, the 3 d compressive strength of the filling body is very sensitive to the response of a single factor. Among them, the order of significance of single factor: solid mass fraction ($F = 11.85$, $P = 0.0021$) > gasification slag content ($F = 1.68$, $P = 0.2077$) > m(c): m(FA) ($F = 1.23$, $P = 0.2778$) > desulfurization gypsum content ($F = 0.68$, $P = 0.4178$).

5. Conclusion

(1) SEM and XRD show that the gasification slag has mainly a honeycomb structure. The main component is SiO_2. Most of the fly ash is of spherical structure, with finer particles. The particle size is mostly distributed below 200 μm, and its composition is SiO_2. Desulfurized gypsum is distributed in a thin-walled and columnar structure, and a small amount of desulfurized gypsum can promote the improvement of early compressive strength. The main component of furnace bottom slag is SiO_2, which is distributed in the combined structure of pores and blocks, and the maximum particle size can reach 25 mm, of which the proportion of furnace bottom slag below 2.5 mm is 56.5%. The main components of coal gangue and cement are SiO_2 and Ca_3SiO_5, respectively. In addition, the particle size of 2.5~5 mm coal gangue and cement accounting for 80.8% is mostly distributed below 100 μm, the overall particle size is small, the pore matching effect is better after mixing, and the microstructure of cement is significantly different from that of a variety of solid wastes.

(2) In view of the combination of bulk coal-based solid waste disposal and green filling mining in the Ningdong mining area, according to experience, 29 groups of proportioning schemes with four factors and three levels of mass fraction (X_1), gasification slag content (X_2), m(c): m(FA) (X_3), and desulfurization gypsum content (X_4) are designed by using the interface response method. The flow characteristics and intensity characteristics of each group are analyzed. The mix proportion of 29 groups of filling materials is divided into high and low uniaxial compressive strength, and 13 groups of high-strength mix proportion are obtained, with the expansion of 200–250 mm. The compressive strength grade is 0.6–1.4 MPa, the flow characteristics and compressive strength characteristics of filling materials are analyzed together, the inclined ladder area obtained by uniaxial compressive strength and expansion is acquired, and six groups of optimal proportion schemes are obtained. At the same time, it is concluded that the compressive strength of filled test blocks at different ages increases with the increase in age, and the higher the mass fraction, the higher the compressive strength. The microscopic test of typical filling test blocks is carried out by SEM. Under the action of cement, the hydration products produced by hydration reaction are different. Meanwhile, a small increase in the content of desulfurized gypsum can significantly improve the cementation performance of the cement. The abundance of rod and flocculent hydration products promotes the compressive strength of filling materials. The law of compressive strength is demonstrated, which shows that it is more reliable and stable when used in coal mine paste filling.

(3) Comprehensive analysis results show that combined with the response surface method, a single factor has a significant effect on the early compressive strength of the consolidated body at the age of 3 d. The order of significance of each factor is solid mass fraction > gasification slag content > m(c): m(FA) > desulfurization gypsum content. The optimal proportioning scheme is obtained through the design, analysis, and prediction of the central group. The mass fraction is 84%, C: FA is 1 : 5, the content of gasification slag is 15%, the content of desulfurization gypsum is 7%, the content of coal gangue is 10%, and the content of furnace bottom slag is 5%. The supplementary experimental results show that σ_{3d} is 1.35 MPa and the expansion is 200 mm. It provides basic parameters for large-scale utilization of coal-based solid waste, especially gasification slag.

Data Availability

The data that support the findings of this study are available from the corresponding author upon reasonable request.

Conflicts of Interest

The authors declare that they have no conflicts of interest.

Acknowledgments

This work was supported by the National Key Research and Development Program of China (2019YFC1904300), the Institute of Energy, Hefei Comprehensive National Science Center under Grant Nos. GXXT-2020-008 and IE-KYXM-015, the University Synergy Innovation Program of Anhui Province (GXXT-2021-017), and the Basic Research on Underground Utilization of Coal Gangue Based Functional Materials (52130402).

References

[1] Q. Q. Qian, F. R. Kang, K. Y. Zhang, X. Zhang, S. L. Wang, and X. Y. Liu, "Research Progress on ecological utilization of coal based solid waste," *Journal of Yulin University*, vol. 31, no. 6, pp. 57–62, 2021.

[2] T. Wei and L. X. Wu, "Restrictive factors and suggestions for the development of modern coal chemical industry in Ningxia," *Research on coal economy*, vol. 41, no. 4, pp. 65–69, 2020.

[3] X. Y. Han and R. A. Liu, "Study on comprehensive utilization, Storage and Disposal Countermeasures of Industrial Solid Waste in East Base," *Resource conservation and environmental protection*, vol. 5, pp. 66-67, 2015.

[4] Y. S. Tang, L. F. Zhang, and H. Y. Lv, "Experimental study on Optimization of filling material ratio for preparation of coal based solid waste," *Journal of Mining Science*, vol. 4, no. 4, pp. 327–336, 2019.

[5] S. J. Wang, "Analysis on present situation and application trend of comprehensive utilization of ash and slag in Ningdong," *Energy Technology*, vol. 18, no. 8, pp. 93–95, 2020.

[6] X. J. Huo and C. Lu, "Influence of mineral composition and fineness of Portland cement on durability of concrete," *People's Yangtze River*, vol. 51, no. S2, pp. 294–296, 2020.

[7] B. Bai, Q. Nie, Y. Zhang, X. Wang, and W. Hu, "Cotransport of heavy metals and SiO2 particles at different temperatures by seepage," *Journal of Hydrology*, vol. 597, Article ID 125771, 2021.

[8] B. Bai, G.-C. Yang, T. Li, and G.-S. Yang, "A thermodynamic constitutive model with temperature effect based on particle rearrangement for geomaterials," *Mechanics of Materials*, vol. 139, Article ID 103180, 2019.

[9] MOHURD, *JGJ/T 70-2009, "Standard for test methods for basic properties of building mortar"*, Ministry of Housing and Urban-Rural Development, Beijing, China, 2009.

[10] Z. D. Cui and H. H. Sun, "Preparation and properties of coal gangue cementitious paste like filling material," *Journal of coal*, vol. 35, no. 6, pp. 896–899, 2010.

[11] Y. X. Wang and Y. C. Yin, "Solid waste in the "Golden Triangle" of energy and chemical industry has become a treasure, starting the "turnaround" of ecological governance," *Science and Technology Daily*, vol. 6, 2021.

[12] M. G. Qian, J. L. Xu, and X. X. Miu, "Green mining technology of coal mine," *Journal of China University of Mining and Technology*, vol. 4, pp. 5–10, 2003.

[13] C. Z. Zhao, H. Q. Zhou, J. B. Bai, and H. Qiang, "Analysis of factors affecting the strength of paste filling materials," *Journal of Liaoning Technical University*, vol. 6, pp. 904–906, 2006.

[14] Q. W. Sun, H. Zhu, and Z. L. Cui, "Preparation and properties of fly ash coal gangue based cemented filling material," *Chinese Journal of Safety Science*, vol. 22, no. 11, pp. 74–80, 2012.

[15] A. X. Wu, Y. Wang, and H. J. Wang, "Present situation and trend of paste filling technology," *Metal Mine*, vol. 7, pp. 1–9, 2016.

[16] K. Cheng, B. G. Yang, B. G. Zhang, D. Li, J. Yang, and R. Zhang, "Present situation and development direction of filling mining technology in coal mines in China," *Coal Technology*, vol. 37, no. 3, pp. 73–76, 2018.

[17] Y. F. Dou, F. Liu, and W. H. Zhang, "Comparative analysis of response surface modeling methods," *Journal of Engineering Design*, vol. 5, pp. 359–363, 2007.

[18] L. Li, S. Zhang, Q. He, and X. B. Hu, "Application of response surface method in experimental design and optimization," *Laboratory research and exploration*, vol. 34, no. 8, pp. 41–45, 2015.

[19] S. L. Liu, G. C. Li, G. L. Liu et al., "Optimization of proportion of slag based solid waste cementitious materials based on response surface methodology," *Silicate Bulletin*, vol. 40, no. 1, pp. 187–193, 2021.

[20] C. Zhang, X. L. Wang, S. G. Li, C. Liu, J. H. Xue, and H. Liu, "Optimization of modified alkali liquor ratio for hydrogen sulfide treatment in Coal Mine Based on response surface method," *Journal of coal*, vol. 45, no. 8, pp. 2926–2932, 2020.